

Article

# On the Cold Deformation Behaviour of Two Phase TiAl Alloy with and without Void Defects

Firstname Lastname<sup>1,†,‡</sup>, Firstname Lastname<sup>1,‡</sup> and Firstname Lastname<sup>2,\*</sup>

<sup>1</sup> School of Mechanical and Electronical Engineering, Lanzhou University of Technology, Lanzhou 730050, China; e-mail@e-mail.com

<sup>2</sup> Affiliation 2; e-mail@e-mail.com

\* Correspondence: e-mail@e-mail.com; Tel.: +x-xxx-xxx-xxxx

† Current address: Affiliation 3

‡ These authors contributed equally to this work.

Version October 2, 2018 submitted to Journal Not Specified

**Abstract:** Fracture processes of nanocrystalline metallic materia is affected by dislocation, nanovoid and other defects. Existing studies of defect evolution in titanium-aluminium alloy cover the case that voids located in single crystals, inside grain in poly crystals and at the grain boundaries. Molecular dynamics simulation was performed to study the evolution of a spherical nanovoid in  $\alpha+\gamma$  two-phase titanium-aluminium alloy under uniaxial tension. The results show that voids located at the  $\alpha/\gamma$  phase boundary have significant detract to strength of Ti-Al polycrystalline.

**Keywords:**  $\alpha + \gamma$  two phase TiAl alloy; void; molecular dynamics

8

- 9 1. Vu, T.T.; Zehender, T.; Verheijen, M.A.; Plissard, S.R.; Immink, G.W.G.; Haverkort, J.E.M.; Bakkers, E.P.A.M. High optical quality single crystal phase wurtzite and zincblende InP nanowires. *Nanotechnology* **2013**, *24*, 115705. doi:10.1088/0957-4484/24/11/115705.
- 10 2. Kim, Y.W. Effects of microstructure on the deformation and fracture of  $\gamma$ -TiAl alloys. *Materials Science and*
- 11 *Engineering: A* **1995**, *192-193*, 519–533. doi:10.1016/0921-5093(94)03271-8.
- 12 3. Xiong, L.; Xu, S.; McDowell, D.L.; Chen, Y. Concurrent atomistic-continuum simulations of dislocation-void
- 13 interactions in fcc crystals. *International Journal of Plasticity* **2015**, *65*, 33–42. doi:10.1016/j.ijplas.2014.08.002.

## 16 1. Introduction

17 TiAl alloy has been used as structural material in aviation industry because its inherent advantages  
18 such as low density and self-diffusion rates, high elastic module and high strength [1]. Two-phase  
19 titanium aluminum alloys with proper phase distribution and grain size exhibit better mechanical  
20 performance compared with monolithic constituents  $\gamma$ (TiAl) and  $\gamma$ (Ti<sub>3</sub>Al) alloy [2]. Brittle fracture in  
21 TiAl alloy strongly affects the safety of fracture of structure like turbo of aircraft engine and combustion  
22 generator.

23 Deformation phenomena in TiAl alloys have been widely studied in order to overcome the  
24 problems associated with the limited ductility and damage tolerance. The literature data covers a  
25 wide range of parameters such as alloy composition, microstructure and deformation temperature.  
26 Much of the work has been performed on single phase  $\gamma$  alloys and PST crystals. Rupture failure at  
27 the macroscopic scale can be attributed to nucleation, growth and propagation of cracks, but at the  
28 microscopic scale cracks are initially easily formed at defects in the casting process, such as voids  
29 and inclusions [3]. These defects are known to play a fundamental role in the deformation of the  
30 material. Nucleation, growth and coalescence of voids are deemed as the primary mechanism of

31 ductile material fracture, in which void growth is particularly important. Therefore, it is necessary to  
 32 study the deformation response of porous materials with the consideration of microstructure evolution.

33 Brittle fracture in TiAl alloy strongly affects the safety of fracture of structure like turbo of aircraft  
 34 engine and combustion generator [1]. Defects such as grain boundary, void and segregation plays an  
 35 significant role in the process of fracture [2]. In order to understand the mechanism of brittle fracture,  
 36 multi-scale methods from micro to macro scale have been applied to investigate the behavior of  
 37 fracture. It's necessary to carefully examine the evolution of defects and its influence on the fracture  
 38 process at atomic scale. A previous study on void growth in gamma-TiAl single crystal has revealed that  
 39 void with high volume fraction detracts incipient yield strength [3]. Molecular dynamics (MD) method  
 40 has been used to investigate the evolution of void in materials in nanoscale [4]. The fracture mechanisms  
 41 in the duplex micro-structure are plasticity induced grain boundary decohesion and cleavage, while  
 42 those in the lamellar microstructure are interface delamination and cracking across the lamellae [5].

43 MD simulations reveals that existence of voids alone may contribute to strain hardening  
 44 because they are barriers to dislocation movement [3].

## 45 2. Molecular Dynamics Simulation

### 46 2.1. Atomic Potential

47 The interaction of particle in the material is determined by interatomic potential. Many reported  
 48 examples of crack propagation in metal materials were performed with embedded atom method  
 49 due to its better accuracy in metal lattice compared with F-S and L-J [6]. The embedded atom method  
 50 (MEAM) potential developed by Zope and Mishin [7] was used in the study. The simulation is  
 51 submitted by MD simulations with the Large-scale Atomic/Molecular Massively Parallel Simulator  
 52 (LAMMPS) open-source code [8]. We performed constant-pressure and constant-temperature (NPT)  
 53 molecular dynamics simulation.

$$E_{total} = \sum F_i(\rho_{h,i}) + \frac{1}{2} \sum_i \sum_{j \neq i} \phi_{ij}(R_{ij}) \quad (1)$$

54 where  $E_{total}$  is the total energy of the system,  $\rho_{h,i}$  is the host electron density at atom  $i$  due to the  
 55 remaining atoms of the system,  $F_i(\rho)$  is the energy for embedding atom  $i$  into the background electron  
 56 density  $\rho$ , and  $\phi_{ij}(R_{ij})$  is the core-core pair repulsion between atoms  $i$  and  $j$  separated by the distance  
 57  $R_{ij}$ . It can be noted that  $F_i$  only depends on the element of atom  $i$  and  $\phi_{ij}$  only depends on the elements  
 58 of atoms  $i$  and  $j$ . The electron density is, as stated above, approximated by the superposition of atomic  
 59 densities, namely

### 60 2.2. Model Creation of Crystalline

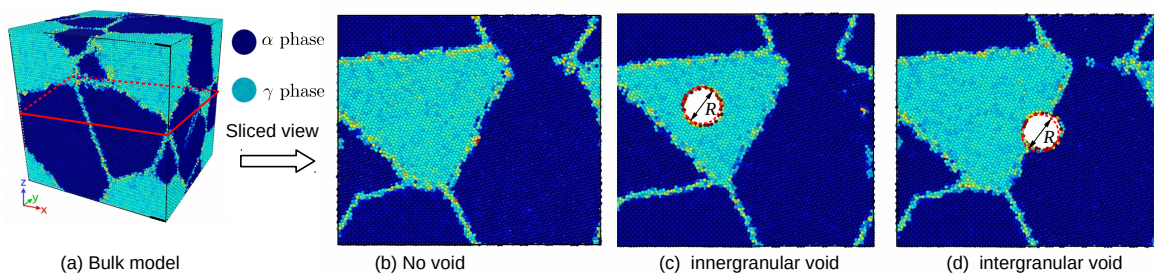


Figure 1. Overview of model creation

61 [9]  $\gamma$  TiAl has a fcc-centered tetragonal with an  $L1_0$  structure [10], and  $\alpha$ -TiAl is hcp structure, the  
 62 structure of the two initial cells are shown in Fig. [11], and the constructing parameters are given by Table. [12].  
 63 The simulation cells of two phase polycrystalline with an initially spherical void at different position

are shown in figure [1]. Periodic boundary conditions (PBC) are applied along all three directions, that makes poly crystal with periodic nanovoid structures. The initial dimension of simulation cell is  $L_x = \text{nm}$ ,  $L_y = \text{nm}$ ,  $L_z = \text{nm}$ , and each model contains about 4.6 million atoms. The grain orientation and size were randomly created with Voronoi method with code ATOMSK [1], and resulting in the arbitrary shape and orientation of the grains. Only one spherical void defect was placed intragranularly or intergranularly within each simulation model void within each simulation model. The intragranular spherical void was located in grain interior of the largest grain of the simulation model, as shown in Fig. [1]. The intergranular spherical void was at the center of the simulation cell, as shown in Fig. [1].

**Table 1.** Parameters of nanocrystalline

Phase	Space group	Designation	Parameters
$\alpha_2$	P6 <sub>3</sub> /mmc	O <sub>19</sub>	$a = 0.5765$ $c = 0.46833$
$\gamma$	tP4	L1 <sub>0</sub>	$a = 0.3997$ $c = 0.4062$

### 2.3. Analysis method

The centrosymmetry parameter is defined as follow:

$$P = \sum_{i=1}^6 |\vec{R}_i + \vec{R}_{i+6}|^2 \quad (2)$$

where  $\vec{R}_i$  and  $\vec{R}_{i+6}$  are the vectors corresponding to the six pairs of opposite nearest neighbors in the fcc lattice. The centrosymmetry parameter(CSP) is zero for atoms in a perfect lattice. In other words, if the lattice is distorted the value of P will not be zero. Instead, the parameter will have a value within the range corresponding to a particular defect. By removing all the perfect and surface atoms within the bulk, the existence of dislocation atoms become visible.

### 3. Results and Discussion

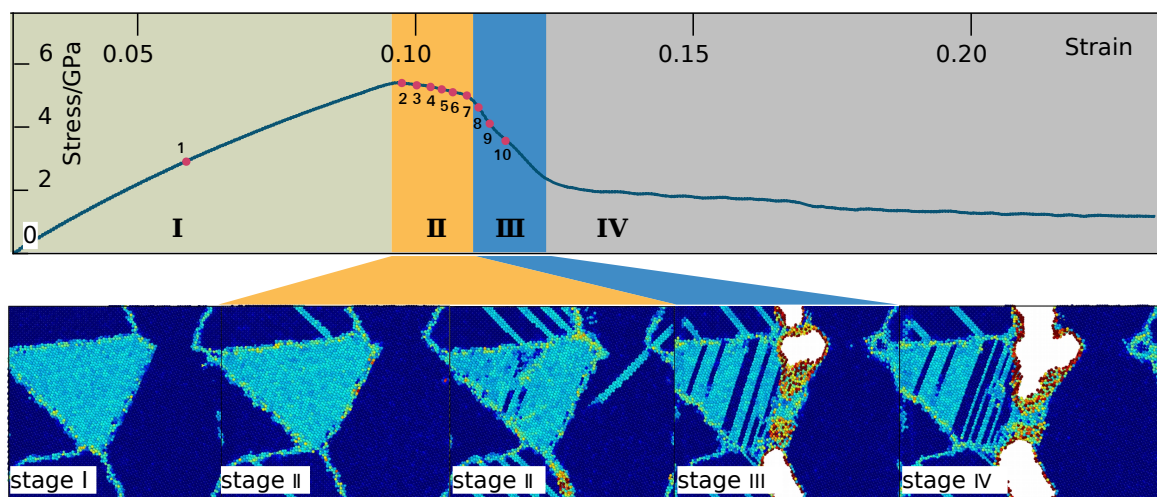


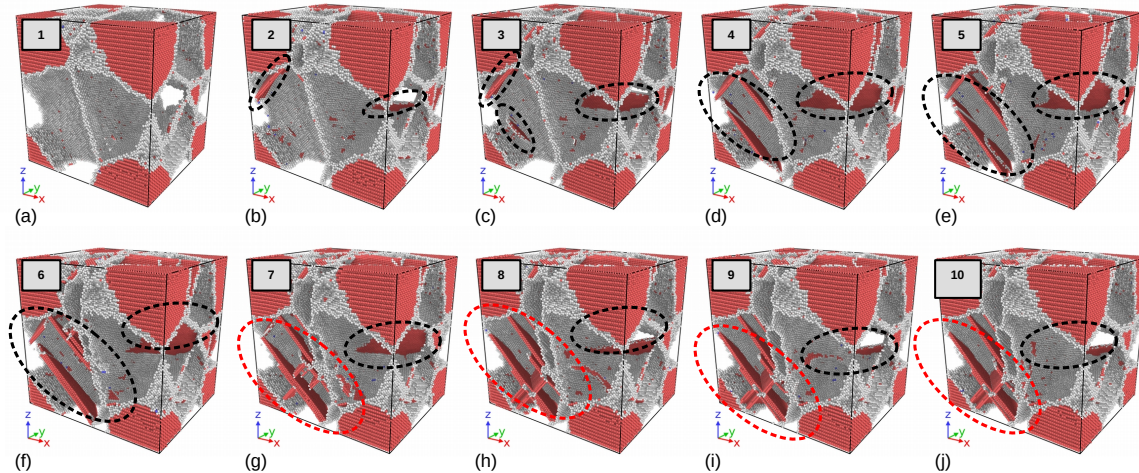
**Figure 2.** perfect-line2-2

**Table 2.** Key point during tensile process

Key Number	1	2	3	4	5	6	7	8	9	10
Time/ps	0	0.15	0.16	0.17	0.18	0.19	0.20	0.21	0.22	0.23
Strain	0	0.15	0.16	0.17	0.18	0.19	0.20	0.21	0.22	0.23

### 79 3.1. Deformation Behaviour of Two Phase Alloys without Void Defects

80 However, the following discussion concentrates on deformation phenomena that rely on the  
 81 elastoplastic codeformation of the  $\gamma$  and  $\gamma_2$  phases and on the particular point defect situation occurring  
 82 in twophase alloys. Due to this effect ( $\alpha_2 + \gamma$ ) alloys exhibit some remarkable properties that are  
 unlike those of either constituent. The configure of atoms is shown in Fig.5, it can be seen that

**Figure 3.**  $\gamma$  phase deformation

83 dislocation emission initiate in  $\gamma$  pahse in XXX ps, and the deformation canbe mainly confied to the  
 84 majority  $\gamma$  pahse.  $\gamma$ (TiAl) deforms by octahedral glide of ordinary dislocations with the Burgers  
 85 vector  $b=1/2<110]$  and superdislocations with the Burgers vectors  $b=<101]$  and  $b = 1/2 < 11\bar{2}]$ . The  
 86 other potential deformation mode is mechanical twinning along  $1/6 < 11\bar{2}]111$ . From Fig.5, of the  
 87 two constituents of  $(\alpha_2+\gamma)$  alloys, the  $\alpha_2$  phase is more difficult to deform. A reason for the unequal  
 88 strain partitioning between the  $\alpha_2$  and  $\gamma$  phase is certainly the strong plastic anisotropy of the  $\alpha_2$   
 89 phase. TEM examinations performed on tensile tested lamellar alloys have revealed that the limited  
 90 plasticity of the  $\alpha_2$  phase is mainly carried by local slip of  $<\alpha>$ -type dislocations with the Burgers vector  
 91  $b = 1/3 < 11\bar{2}0 >$  prism planes<sup>5</sup>, which is by far the easiest slip system in  $\alpha_2$  single crystals. Basic  
 92 deformationg mechanism of  $\alpha$  phase

93 1.In many cases the orientation of slip slip is changed because the crystallographically available  
 94 slip and directions are not continuous across the interface. This may significantly reduce the Schmid  
 95 factor and thus impede slip transfer. At the  $\gamma/\gamma$  interfaces the orientation of the slip plan could change  
 96 through a relevantly large angle of about 90 degree. Reorientation of slip is always required at the  
 97  $\alpha_2/\gamma$  interface; the smallest angle between the corresponding slip planes  $111_\gamma$  and  $10 - 10_{\alpha_2}$  is about  
 98 19 degree [].

99 The core of a dislocation intersecting an interface often needs to be transformed. For example, an  
 100 ordinary  $1/2<110]$  dislocation gliding in one  $\gamma$  grain has to be converted in to a  $<101]$  super dislocation  
 101 with the double Burgers vector gliding in an adjacent  $\gamma$  grain. At the  $\alpha/\gamma$  interface the dislocations  
 102 existing in the  $D0_{19}$  structure have to be transformed into dislocations consistent with the  $L1_0$ structure.  
 103 These core transformations are associated with a change of the dislocation line energy because the  
 104 lengths of the Burgers vectors and the shear module are different.

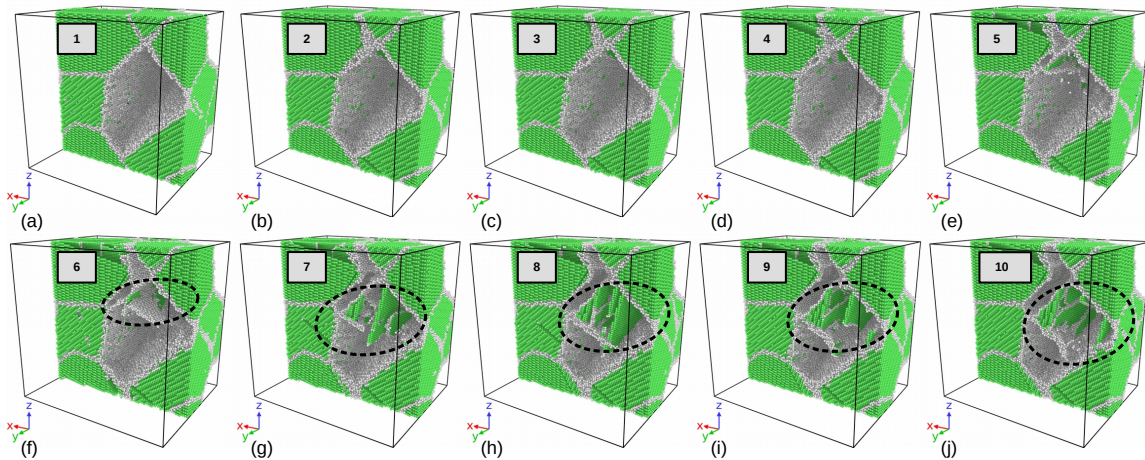


**Figure 4.**  $\alpha$  phase deformation

106 Dislocations crossing semi-coherent boundaries have to intersect the misfit dislocations, a process  
 107 that involves elastic interaction, jog formation and the incorporation of gliding dislocations into the  
 108 mismatch structure of the interface. When the slip is forced to cross  $\alpha_2$  lamella, pyramidal slip of the  $\alpha_2$   
 109 phase is required, which needs an extremely high shear stress.

110 *3.2. Evolution of spherical void in the simulation with intragranular spherical voids*

111 The volume defects considered pertain to three-dimensional objects contained within a matrix.  
 112 Three-dimensional structures composed of zero-, one- or two-dimensional defects are not considered  
 113 here. Second-phase particles, precipitated within, as a consequence of a thermal treatment, or taken  
 114 up, as a consequence of a material processing route, into a matrix of the first, dominant phase, disrupt,  
 115 more or less (as possibly associated with the occurrence of incoherent or coherent interfaces; see Sect.  
 116 5.3), the long-range translation symmetry of the matrix. They may induce considerable misfit-stress  
 117 fields and thus can influence material properties pronouncedly. Such stress fields surrounding the  
 118 second-phase particles can be due to misfit between the volume occupied by the second-phase particle  
 119 when unconstrained and the space ("hole") put at its disposal by the matrix. Such misfit can arise  
 120 due to specific volume differences induced by precipitation or by different thermal expansion or  
 121 shrinkage upon heating or cooling the specimen. A possibly favourable effect of second-phase particles  
 122 is a contribution to the enhancement of mechanical strength. Considering yielding of a material as  
 123 related to glide of dislocations (Sect. 5.2.5), any mechanism obstructing dislocation glide improves the  
 124 mechanical strength. In the discussion of the Frank–Read source for dislocation (-line) production (Sect.  
 125 5.2.6) it was made clear that second-phase particles can serve as obstacles for dislocation migration:  
 126 the stress fields surrounding the second-phase particles can be of "antagonistic" nature and "block"  
 127 propagation of the stress field of a migrating dislocation: the second-phase particle acts as "pinning  
 128 point". It was already indicated that in order that a dislocation can pass two pinning points (A and B  
 129 in Fig. 5.13; see Sect. 5.2.6) a critical shear stress is needed that depends on the distance between the  
 130 obstacles (which can be second-phase particles):

$$\tau_0 = Gb/d \quad (3)$$

131 where  $d$  represents the distance between A and B and thus reflects the dependence of the critical  
 132 shear stress  $\tau_0$  on the second-phase particle density and distribution. This mechanism for hardening is  
 133 designated as the Orowan process (with  $\tau_0$  as the Orowan (shear) stress ; see also Sect. 11.14.4). As a  
 134 result of the Orowan process, upon passage of the pinning points by a series of gliding dislocations, a  
 135 system of concentric loops is formed around the second-phase particles (see Fig. 5.27). Consequently,

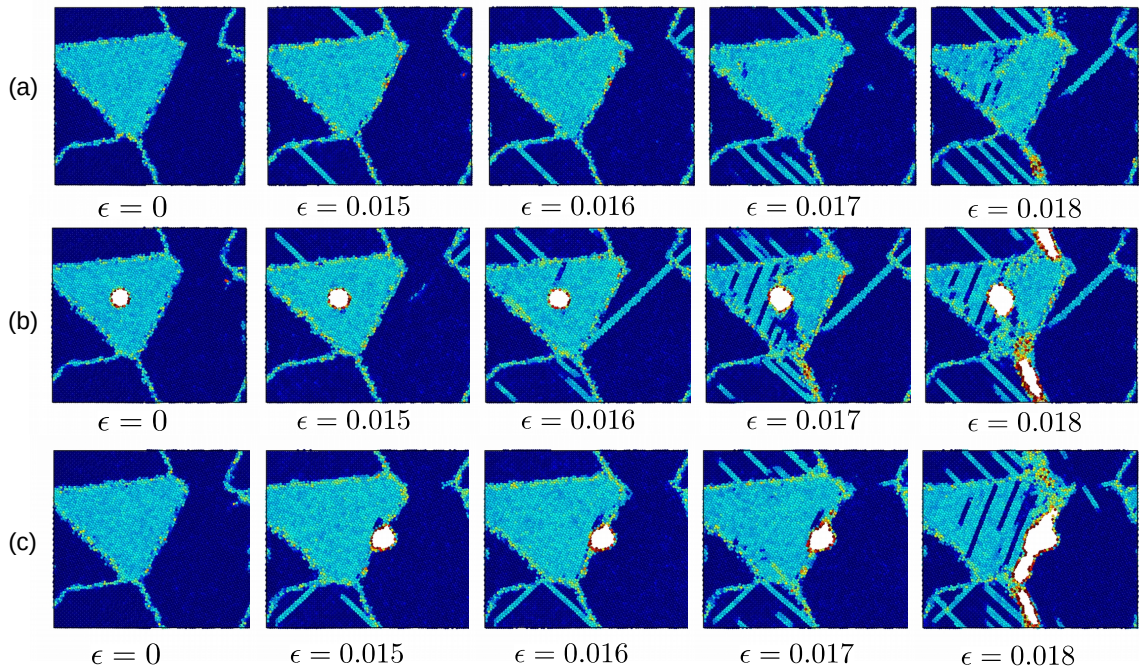


**Figure 5.** Yield process of the models

the effective average distance between the second-phase particles has decreased to  $d$  which implies a necessary increase of the value of critical shear stress required for continuation of dislocation glide (cf. (5.10)). A step, of the width of a burgers vector, will be generated at both sides of a crystal along the direction of the burgers vector after dislocation traversing the entire crystal, as is shown in ???. A small step will be formed at spherical void surface toward the void interior after dislocation absorption at spherical void surfaces, as is shown in ???. If a great number of dislocation slip along their respective systems towards the spherical nanovoid in all directions, and are absorbed at spherical void surfaces, the spherical nanovoid will eventually shrink from the dash circle to

### 3.3. The effect of void on the strength of material

Void of  $R=10$  was placed at phase boundary, inside  $\alpha$  phase grain respectively. Effect of void at different position under uniaxial tension is shown in Fig.10. The strength of materials with void in different size and at different position is shown in Fig.10. The results show that the model without void defect has best strength, while the void located inside  $\alpha$  phase detracts the strength of the material most, and the void at the phase boundary have less impact on the strength.

The effect of size is expectable that the greater voids detracts the strength of the materials more, however, it has been observed in the simulation that there is a critical value about  $15\text{A}$  for voids at different position. The voids larger than  $15\text{ A}$  have dramatic detraction to the strength of the material. Conventional definition of strength of materials with geometry subtraction was applied to the model, and theoretical strength of the models was calculated by formulation 4:

$$\sigma^* = \sigma_0 \cdot \frac{A^*}{A_0} \quad (4)$$

where  $\sigma_0$  is the strength of the model without void defects  $5.26\text{ Gpa}$ , and  $A_0$  is initial section area,  $A = a \times b = 36000\text{A}^2$ ,  $A^*$  is section area in consideration of the subsection that results from the voids. Comparing with the strength determined by molecular dynamics simulation and the results calculated with formulation 4, it can be assumed that the main factor that affects the strength of materials can be attributed to local behaviour of the materials, thus revolution of defects should be examined carefully.

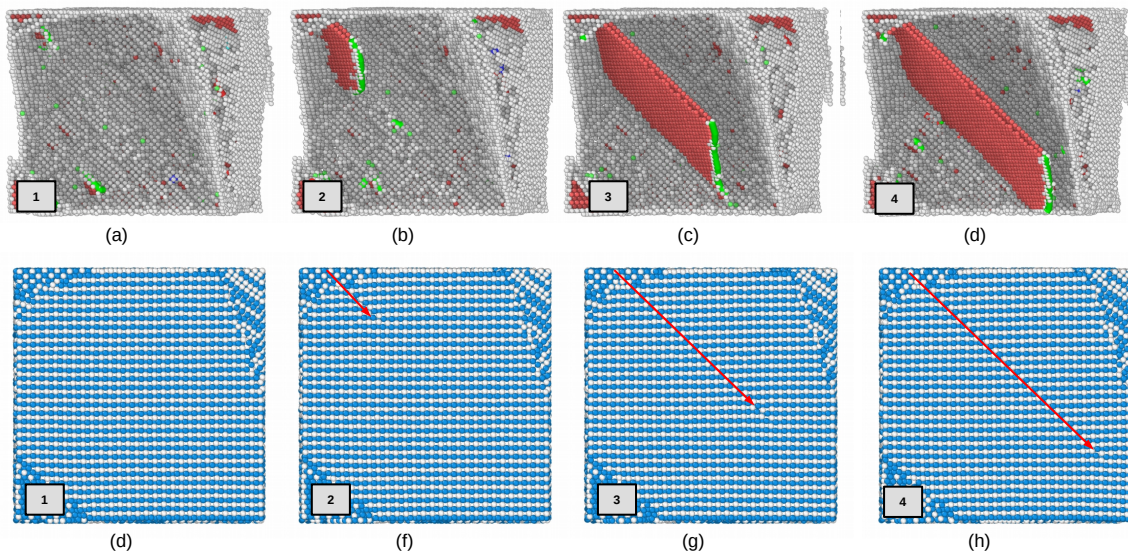


**Figure 6.** Dislocation in  $\gamma$

Voids with different size: 2A, 5A, 10A, 15A were placed into the model respectively. It has been observed that voids detracts the strengths of the material. The max stress stress of the simulation cell decreases as the volume of voids are lareger. From Fig ??, there is a critical value of void radius about 15A, the void greater than 15A cause serious detraction of strength of material. Engineering stress is calculated

$$\sigma = S / A$$

160 The rate of decrease of loading area are smaller comparing with the detraction of strength, so it can  
 161 be assumed that the yield yield behaviour and strength is much more related with local behaviour of  
 162 grain boundaries and void.

163 Grain and phase boundaris are obstacles to deformation process, thus the stability of boundaries  
 164 have great impact on the strength of materials. Interactive between grainboundary and void determines  
 165 the fracture mode of the TiAl alloy.

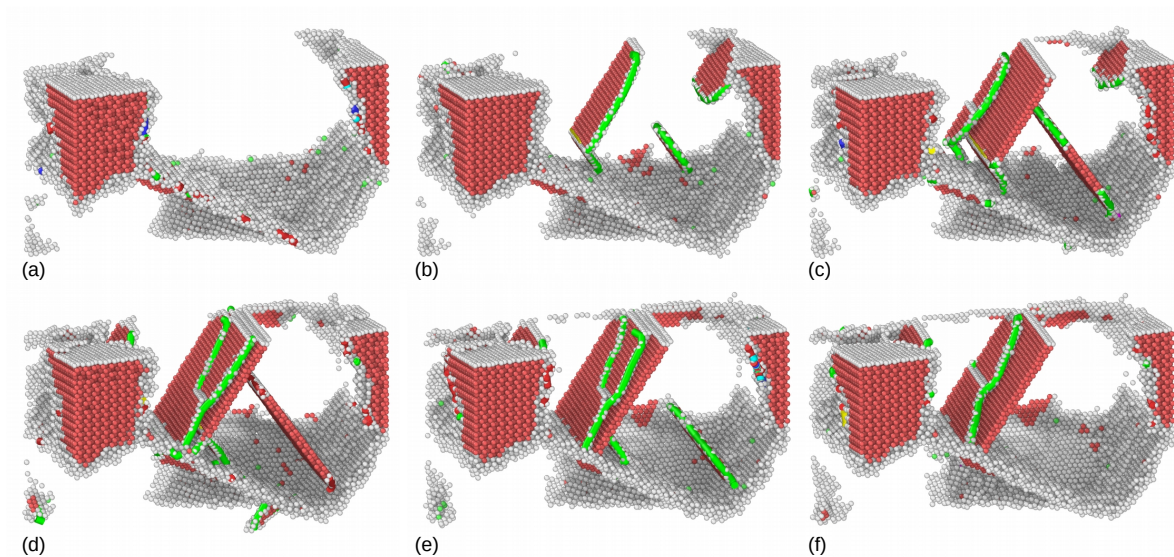
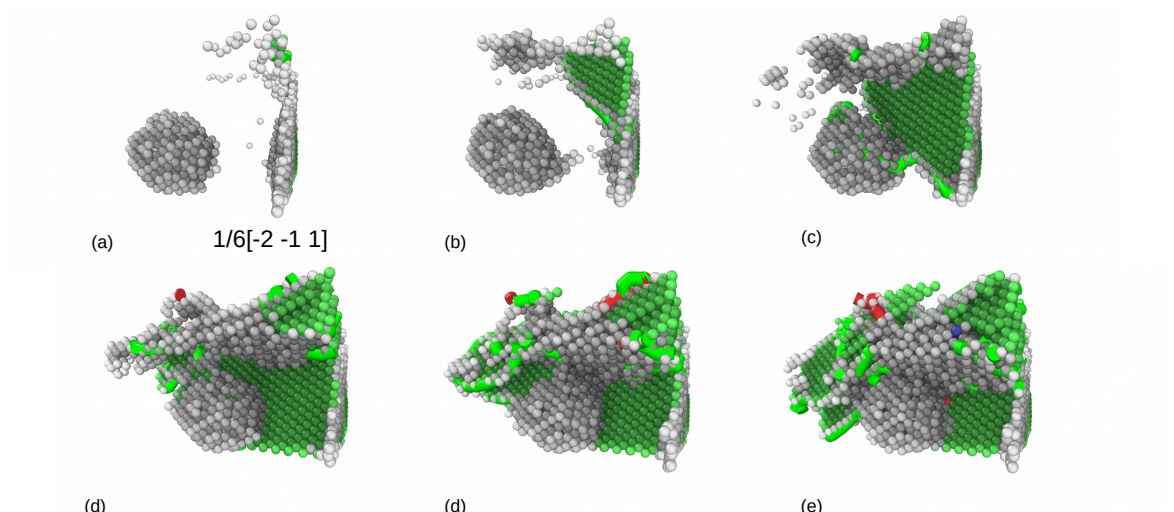
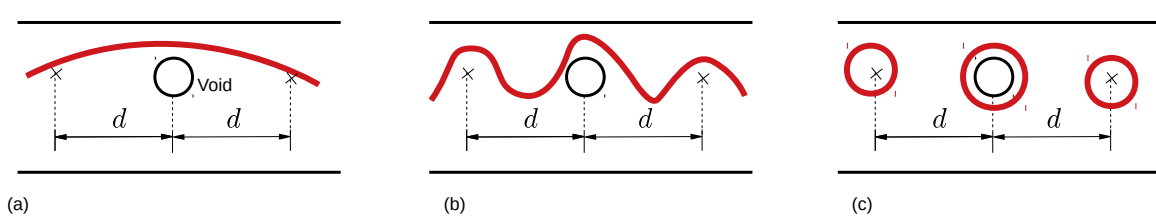
According to Schmid's law:

$$\tau = \sigma * m$$

where m is the Schmid factor :

$$m = \cos(\phi)\cos(\lambda)$$

166 © 2018 by the authors. Submitted to *Journal Not Specified* for possible open access  
 167 publication under the terms and conditions of the Creative Commons Attribution (CC BY) license  
 168 (<http://creativecommons.org/licenses/by/4.0/>).

**Figure 7.** stress-strain curve**Figure 8.** Dislocation around void**Figure 9.** orowan

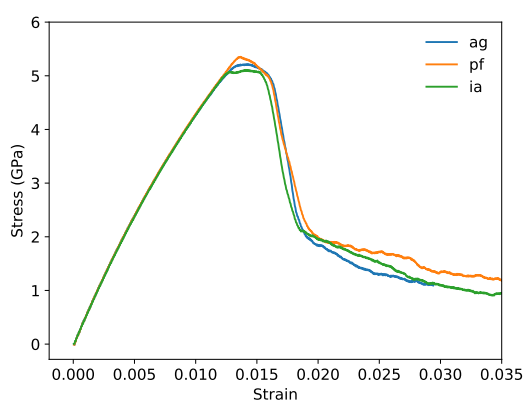


**Figure 10.** Stress-Strain

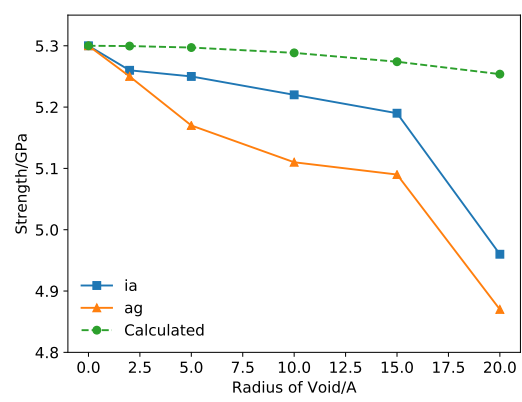


**Figure 11.** Strength of models